



## Orrorin tugenensis Femoral Morphology and the Evolution of Hominin Bipedalism

Brian G. Richmond, *et al.*  
*Science* **319**, 1662 (2008);  
DOI: 10.1126/science.1154197

**The following resources related to this article are available online at [www.sciencemag.org](http://www.sciencemag.org) (this information is current as of March 27, 2008 ):**

**Updated information and services**, including high-resolution figures, can be found in the online version of this article at:

<http://www.sciencemag.org/cgi/content/full/319/5870/1662>

**Supporting Online Material** can be found at:

<http://www.sciencemag.org/cgi/content/full/319/5870/1662/DC1>

A list of selected additional articles on the Science Web sites **related to this article** can be found at:

<http://www.sciencemag.org/cgi/content/full/319/5870/1662#related-content>

This article **cites 31 articles**, 6 of which can be accessed for free:

<http://www.sciencemag.org/cgi/content/full/319/5870/1662#otherarticles>

This article appears in the following **subject collections**:

Anthropology

<http://www.sciencemag.org/cgi/collection/anthro>

Information about obtaining **reprints** of this article or about obtaining **permission to reproduce this article** in whole or in part can be found at:

<http://www.sciencemag.org/about/permissions.dtl>

packing also imparts protection from current damage and/or high-energy events and allows for selection of most favorable sites for attachment and growth to adulthood (12).

Aggregation is not uncommon among some elements of the Ediacaran biota and is present in the frond holdfast *Aspidella*. These typically occur in dense assemblages, but in contrast to *F. dorothea*, their size distribution is consistent with continuous recruitment (1, 13, 14) rather than periodic cohort growth. The terminal Neoproterozoic calcified tubes *Cloudina* and *Namacalathus* also show evidence of aggregation (15), but there is no indication of distinct cohorts.

These data demonstrate that even morphologically simple Ediacaran organisms had multiple modes of growth and propagation, reminiscent of several of the most successful marine invertebrate ecological strategies today (16). These systems were in place in Earth's oldest known metazoan ecosystems before the ecological pressures that

accompanied the advent of skeletonization and extensive predation.

#### References and Notes

- M. L. Droser, J. G. Gehling, S. R. Jensen, *Palaeogeogr. Palaeoclimatol. Palaeoecol.* **232**, 131 (2006).
- J. G. Gehling, *Precambrian Res.* **100**, 65 (2000).
- J. G. Gehling, *Palaios* **14**, 40 (1999).
- M. F. Glaessner, *Lethaia* **2**, 369 (1969).
- M. L. Droser, J. G. Gehling, S. R. Jensen, Eds., *Ediacaran trace fossils: Truth and false* (Peabody Museum of Natural History, New Haven, CT, 2005), pp. 125–138.
- D. K. Jacobs, N. C. Hughes, S. T. Fitz-Gibbon, C. J. Winchell, *Evol. Dev.* **7**, 498 (2005).
- J. G. Gehling, M. L. Droser, S. R. Jensen, B. N. Runnegar, Eds., *Ediacara Organisms: Relating Form to Function* (Yale Peabody Museum, New Haven, CT, 2005).
- D. G. Fautin, *Can. J. Zool.* **80**, 1735 (2002).
- J. B. C. Jackson, in *Biotic Interactions in Recent and Fossil Benthic Communities*, M. J. S. Tevesz, P. L. McCall, Eds. (Plenum Press, New York, 1983), vol. 3, pp. 39–120.
- D. J. Crisp, in *Biology and Systematics of Colonial Organisms*, G. P. Larwood, B. R. Rosen, Eds. (Academic Press, New York, 1979), pp. 319–327.
- S. Bengtson, Z. Yue, *Science* **257**, 1645 (1992).
- G. Wörheide, A. M. Solé-Cava, J. N. A. Hooper, *Comp. Biol.* **45**, 377 (2005).
- K. J. Peterson, B. Waggoner, J. W. Hagadorn, *Integr. Comp. Biol.* **43**, 127 (2003).
- J. G. Gehling, G. M. Narbonne, M. A. Anderson, *Palaeontology* **43**, 427 (2000).
- J. E. Anthor et al., *Geology* **31**, 431 (2003).
- L. J. Holts, K. A. Beauchamp, *Mar. Biol.* **116**, 129 (1993).
- This research was supported by a National Science Foundation grant (EAR-0074021) and a NASA grant (NNG04GJ42G NASA Exobiology Program) to M.L.D. and an Australian Research Council Grant (DP0453393) to J.G.G. We are indebted to J. Fargher and R. Fargher for access to their property and permission to excavate fossiliferous beds. Fieldwork was facilitated by D. Rice, S. Jensen, J. Paterson, M. Dzaugis, M. E. Dzaugis, R. Droser, and members of the Waterhouse Club. N. Hughes, R. Wood and S. Xiao provided helpful comments. D. Garson constructed Fig. 2.

#### Supporting Online Material

www.sciencemag.org/cgi/content/full/319/5870/1660/DC1  
SOM Text  
Fig. S1

5 November 2007; accepted 1 February 2008  
10.1126/science.1152595

# *Orrorin tugenensis* Femoral Morphology and the Evolution of Hominin Bipedalism

Brian G. Richmond<sup>1,2\*</sup> and William L. Jungers<sup>3</sup>

Bipedalism is a key human adaptation and a defining feature of the hominin clade. Fossil femora discovered in Kenya and attributed to *Orrorin tugenensis*, at 6 million years ago, purportedly provide the earliest postcranial evidence of hominin bipedalism, but their functional and phylogenetic affinities are controversial. We show that the *O. tugenensis* femur differs from those of apes and *Homo* and most strongly resembles those of *Australopithecus* and *Paranthropus*, indicating that *O. tugenensis* was bipedal but is not more closely related to *Homo* than to *Australopithecus*. Femoral morphology indicates that *O. tugenensis* shared distinctive hip biomechanics with australopiths, suggesting that this complex evolved early in human evolution and persisted for almost 4 million years until modifications of the hip appeared in the late Pliocene in early *Homo*.

Bipedalism is one of very few human characteristics that appears to have evolved at the base of the hominin clade [species more closely related to modern humans than to any other living species (1)]. Recent fossil discoveries have apparently pushed back the origin of the hominin clade into the late Miocene, to 6 to 7 million years ago (Ma). The oldest known potential hominin fossils, attributed to *Sahelanthropus tchadensis*, come from Toros-Menalla in Chad and are biostratigraphically dated to ~7 Ma (2). Currently, *Sahelanthropus* is only known from craniodental evidence, and although the

position of the foramen magnum suggests that it was bipedal (3), postcranial fossils are needed to confirm this conclusion. The next oldest potential hominin remains were discovered in 2000 by Senut, Pickford, and colleagues (4) from localities (5.7 to 6.0 Ma) in the Lukeino Formation in Kenya (5, 6) and attributed to *Orrorin tugenensis*. Of the fossils assigned to *O. tugenensis*, three fragmentary femora (BAR 1002'00, 1003'00, and 1215'00) are critical pieces of evidence because they are interpreted as having derived characteristics indicating bipedalism (7). However, some of these features are also found in non-bipedal primates and are therefore inconclusive (8). Similarly, a study of the femora based on computerized tomography (9) suffered from poor image resolution and does not provide convincing evidence of bipedality (10). The discoverers have also cited the femora in formulating hypotheses about early hominin phylogenetic relationships (4), but these have been disputed (8, 11, 12). Thus, the morphology of the *O. tugenensis* femora

is critical to our understanding of the origin of bipedalism and phylogenetic relationships of the earliest hominin taxa, yet the functional and phylogenetic implications of their morphology remain highly controversial. We present here a quantitative, morphometric (shape) comparison of the most complete *O. tugenensis* femur, BAR 1002'00, of a young adult.

When compared to the proximal femora of a large and diverse sample of great apes, modern humans (including small-bodied adult individuals from African Pygmy and Andaman Island populations), as well as Plio-Pleistocene hominin femora (13), the *O. tugenensis* femur (BAR 1002'00) more closely resembles femora attributed to early hominin taxa (*Australopithecus* and *Paranthropus*) than do those of extant apes, fossil *Homo*, and modern humans. Multivariate analyses of shape (canonical variates, cluster analysis, and principal components analysis) reveal that modern human proximal femora are distinct from those of extant great apes primarily in having a relatively large head and short distance between the head and lesser trochanter. Canonical variates axis 1 (Fig. 1A) is a contrast vector driven by these distinguishing features of shape (table S1), and the non-*Homo* fossil hominins (including BAR 1002'00) occupy an intermediate position in this part of multivariate space. The second axis separates orangutans from African apes, modern humans, and all the fossils. Orangutans have relatively large femoral heads (related to mobility rather than more pronounced weight support) combined with narrow femoral shafts, a combination of features not seen in modern or fossil hominin femora. The third axis, driven by neck length and breadth, and shaft breadth, serves to separate early hominin femora from those of extant apes, modern humans, and fossil *Homo* taxa. BAR 1002'00 resembles the early hominin femora, which are characterized in this and previous analyses by a combination of long and

<sup>1</sup>Center for the Advanced Study of Hominid Paleobiology, Department of Anthropology, The George Washington University, 2110 G Street, NW, Washington, DC 20052, USA. <sup>2</sup>Human Origins Program, National Museum of Natural History, Smithsonian Institution, Washington, DC 20560, USA. <sup>3</sup>Department of Anatomical Sciences, Stony Brook University, Stony Brook, NY 11794-8081, USA.

\*To whom correspondence should be addressed. E-mail: brich@gwu.edu

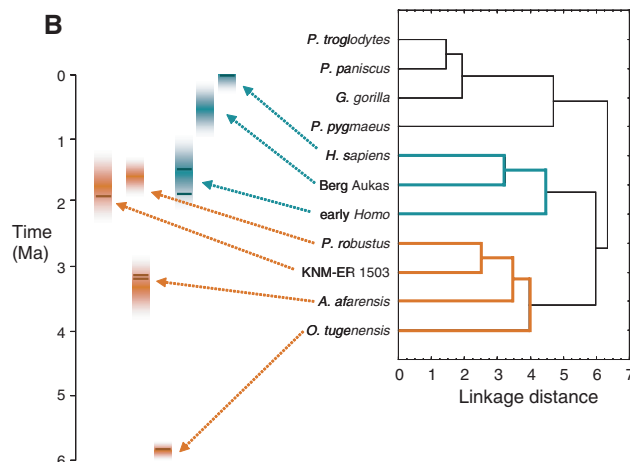
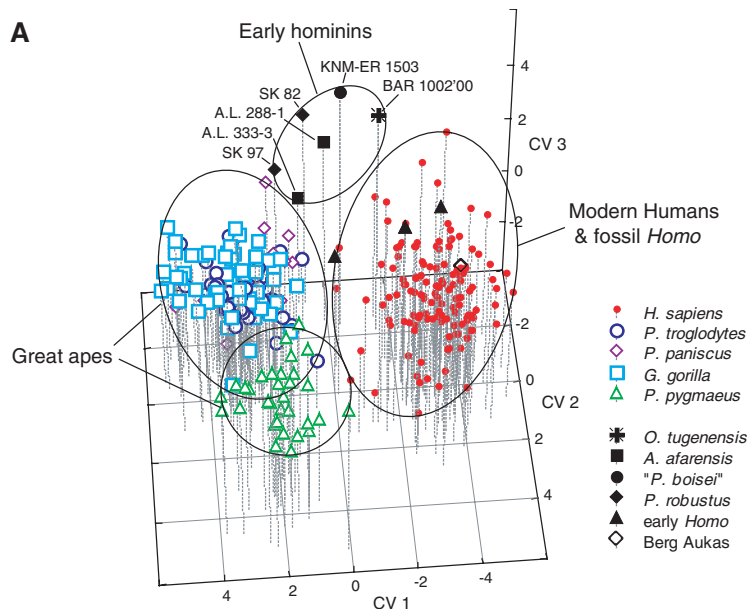
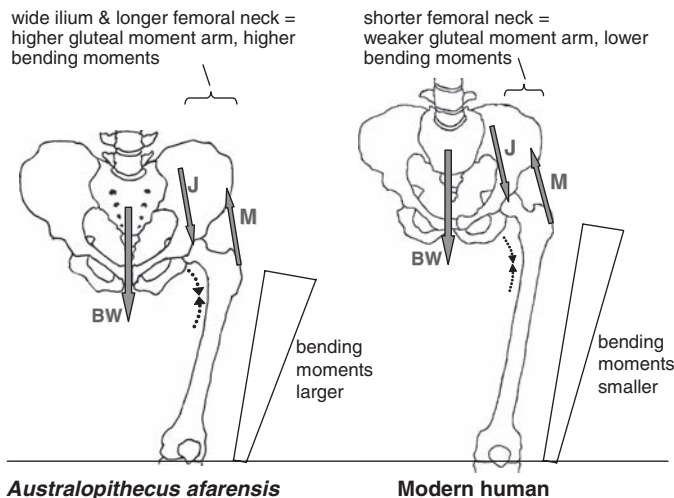


**Fig. 1.** Multivariate analysis of femoral shape among species. **(A)** Canonical variates (CV) analysis of proximal femur shape completely separates modern humans, great apes, and early hominins. BAR 1002'00 most closely resembles KNM-ER 1503. **(B)** Cluster analysis (UPGMA of Mahalanobis  $D^2$  distances) shows three distinct clusters: a

great ape cluster, a cluster of modern and fossil *Homo*, and a cluster of BAR 1002'00 and early hominins. The early hominin femoral morphology exhibited by BAR 1002'00 appears to persist for more than 4 million years, with a major change in hip structure in early *Homo*.

**Fig. 2.** Hominin hip biomechanics. Distinctive features of the early hominin hip (**left**) are part of a biomechanical complex in which the tendency of the body weight force (BW) to pull down the trunk during gait is counteracted by the gluteal muscle force acting on the pelvis. Compared to modern humans (**right**), the wider iliac blade and longer femoral neck of the early hominin hip (**left**) result in greater moment arms for the gluteal muscle force (M).



They also result in greater femoral shaft bending moments from the joint reaction force (J), which in turn are related to greater mediolateral shaft robusticity to withstand the elevated compressive stresses along the medial side of the proximal femoral shaft. Thus, the long femoral neck, wide proximal shaft, and possibly the small femoral head are part of a biomechanical complex. (Vector and bending moment illustrations not to scale.)

anteroposteriorly constricted necks, mediolaterally broad shafts, and smaller heads (relative to modern humans) (14–17). This morphological complex is not merely an allometric consequence of the small size of many of the fossils (fig. S3), including A.L. 288-1 and BAR 1002'00 (18), as the small-bodied modern humans and apes in this sample do not resemble the early hominins. Three distinct clusters summarize these affinities (Fig. 1B); modern humans and fossil *Homo* form a group that is linked to a cluster of *Australopithecus*, *Paranthropus*, and *O. tugenensis*, and these two groups are joined by a more distant cluster of extant apes.

The features (long, narrow neck and broad proximal shaft) characterizing *O. tugenensis* and australopith (19) femora are not biomechanically independent, and reflect differences in hip morphology related to gait mechanics. Modern humans gait is distinct from the kinematics of bipedalism in other primates in several ways, including very little lateral displacement and a slight drop in the contralateral hip during stance phase (20, 21). These characteristics are made possible in part by the flared, short iliac blade and by the recruitment of the lesser gluteal muscles on the ipsilateral side, which counteract the tendency of the body weight force to lower the

contralateral hip (Fig. 2). The very flaring ilia and long femoral necks of australopiths improve the gluteal muscle lever arm and thus counter the torque of body weight (17), but the long necks also increase the bending moment on the proximal femoral shaft. These elevated bending moments are resisted by the greater mediolateral width of the femoral diaphysis, especially proximally where bending moments are highest (22).

*O. tugenensis* shares this uniquely archaic hominin morphological pattern, thus providing strong evidence that *O. tugenensis* was adapted to bipedalism 6 million years ago (Fig. 3). This evidence is functionally consistent with other morphological features believed to be linked to bipedalism in the *O. tugenensis* femora, including a marked obturator externus groove, the presence of an intertrochanteric line, vertical gluteal tuberosity (third trochanter), and a slightly enlarged head (7). BAR 1002'00 bears distinct markings for the medial and lateral extents of the vastus musculature, but it lacks the prominent, raised linea aspera that is distinctive of modern and fossil *Homo* femora. In this manner, BAR 1002'00 resembles some australopith femora [e.g., A.L. 288-1ap (23)]. The relative femoral head size of BAR 1002'00 is intermediate between, and overlaps with, the distribution of *Pan* and *Homo* femora; the femoral head of BAR 1002'00 is large compared to *Australopithecus*, *Paranthropus*, and African ape femora, but relatively smaller than those of orangutans and fossil and modern *Homo* (fig. S6). Furthermore, the difference between BAR 1002'00 and *Australopithecus* and *Paranthropus* in relative femoral head size is within the expected level of intraspecific variation based on extant standards.

To investigate how proximal femur shape has changed over the course of human evolutionary



**Fig. 3.** Morphological comparisons among femora of or attributed to (A) *P. troglodytes*, (B) *O. tugenensis* (BAR 1002'00), (C and D) *Paranthropus robustus* (SK 97 and SK 82, reversed), (E) *A. afarensis* (A.L. 288-1ap), (F) *Paranthropus boisei* (KNM-ER 1503, reversed), (G) early *Homo* (KNM-ER 1481), and (H) modern *H. sapiens*. Like other early hominin femora (C to F), BAR 1002'00 (B) is distinct from those of modern humans (H) and great apes (A) in having a long, anteroposteriorly narrow neck and wide proximal shaft. Early *Homo* femora (G) have larger heads and broader necks compared to early hominins. In addition to these features, modern human femora (H) have short necks and mediolaterally narrow shafts. Scale bar, 2 cm.

history, we plotted against time the multivariate shape Mahalanobis  $D^2$  distance between each femur and the mean shape of *Homo sapiens* femora. Distances are consistently high until the appearance in the late Pliocene and early Pleistocene of femora attributed to *Homo* (fig. S4). The early *Homo* femora retain the primitively long necks and broad shafts (16, 24), suggesting the retention of relatively broad ilia (24), but more closely resemble modern human femora in having larger heads and broader necks. In conjunction with significantly greater femoral length (25), these features provide evidence of a transition to a more modern humanlike bipedal gait including greater speed and energetic efficiency compared to earlier hominins (16, 26–29). Further changes in femoral anatomy (e.g., shorter neck, narrower shaft) occur in the genus *Homo* in the Middle Pleistocene and can be linked in part to obstetrical factors (24).

In light of the marked changes in femoral anatomy from at least 2 Ma to the present, the close morphological similarity between femora of *O. tugenensis* at 6 Ma and *Australopithecus* and *Paranthropus* in the later Pliocene is especially pronounced (Figs. 1 and 3 and table S3). Although among the early hominin taxa, *Ororin* has the smallest Mahalanobis  $D^2$  distance from the modern human centroid, BAR 1002'00 is much closer to all early hominin taxa than to the modern human centroid in shape space (table S3). The external morphology of *O. tugenensis* provides no indications of differences in bipedal gait compared to *Australopithecus* or *Paranthropus*. This suggests that the pattern of bipedal gait characteristic of australopiths evolved very early in the human lineage, and perhaps they were also the characteristics of the first bipedal hominins. This form of bipedalism appears to have

persisted as a successful locomotor strategy for as long as 4 million years (Fig. 1B). Additional lower limb fossils from the late Miocene and early Pliocene will be needed to test this hypothesis.

Similarities in femoral morphology, however, do not rule out possible differences in overall repertoires of positional behavior. Upper limb fossils of *O. tugenensis* retain morphological features related to arboreal climbing, including a pronounced humeral brachioradialis flange and a curved proximal manual phalanx (4). The included angle measured on BAR 349'00 (proximal phalanx) is  $52^\circ$ , significantly greater than those of modern humans and *Macaca mulatta* ( $t$  test,  $P < 0.05$ ), and significantly lower than those of orangutans (fig. S5). In degree of curvature, BAR 349'00 most closely resembles *Pan troglodytes*. The *Pan*-like curvature of the proximal phalanx close to the *Pan-Homo* last common ancestor supports the hypothesis that bipedalism evolved from an ancestor adapted to orthograde and vertical climbing, consistent with a climbing and knuckle-walking repertoire (30), rather than an orangutan-like arboreal specialist (31). Therefore, while *O. tugenensis* was bipedal, it most probably also climbed trees (4), presumably to forage, build nests, and seek refuge. Whether arboreality played a greater role in the locomotor repertoire of *O. tugenensis* in comparison to *Australopithecus* remains unresolved. The available evidence of internal cortical morphology of BAR 1002'00 (7, 9) leaves open the possibility that *O. tugenensis* had a pattern of neck bone cortical thickness that differed from the human-like pattern observed in *Australopithecus* (32) and would be consistent with the use of a wider range of hip joint postures like those used by great apes during climbing. The external anat-

omy of BAR 1002'00 indicates bipedality, but is also consistent with a locomotor repertoire involving an appreciable scansorial component (33, 34).

The similarity between *O. tugenensis* and australopith femora weakens support for scenarios in which *O. tugenensis* is ancestral to *Homo* to the exclusion of *A. afarensis* (4). Instead, the overall primitive hominin morphology of the *O. tugenensis* femur, along with primitive dental anatomy, is consistent with the more parsimonious hypothesis that it is a basal member of the hominin clade. In sum, the comparative biomechanical anatomy of *O. tugenensis* femora suggests that *O. tugenensis* is a basal hominin adapted to bipedalism, and current evidence suggests that an *Australopithecus*-like bipedal morphology evolved early in the hominin clade and persisted successfully for most of human evolutionary history.

## References and Notes

1. B. A. Wood, B. G. Richmond, *J. Anat.* **196**, 19 (2000).
2. M. Brunet *et al.*, *Nature* **434**, 752 (2005).
3. C. P. Zollikofer *et al.*, *Nature* **434**, 755 (2005).
4. B. Senut *et al.*, *C. R. Acad. Sci. Paris Ser. II* **332**, 137 (2001).
5. A. L. Deino, L. Tauxe, M. Monaghan, A. Hill, *J. Hum. Evol.* **42**, 117 (2002).
6. Y. Sawada *et al.*, *C. R. Palevol* **1**, 293 (2002).
7. M. Pickford, B. Senut, D. Gommery, J. Treil, *C. R. Palevol* **1**, 1 (2002).
8. D. R. Begun, *Science* **303**, 1478 (2004).
9. K. Galik *et al.*, *Science* **305**, 1450 (2004).
10. J. C. Ohman, C. O. Lovejoy, T. D. White, *Science* **307**, 845 (2005).
11. L. C. Aiello, M. Collard, *Nature* **410**, 526 (2001).
12. C. J. Cela-Conde, F. J. Ayala, *Proc. Natl. Acad. Sci. U.S.A.* **100**, 7684 (2003).
13. Materials and methods are available as supporting material on Science Online.
14. M. H. Day, *Nature* **221**, 230 (1969).
15. A. C. Walker, *J. Hum. Evol.* **2**, 545 (1973).
16. H. M. McHenry, R. S. Corruccini, *Am. J. Phys. Anthropol.* **49**, 473 (1978).
17. C. O. Lovejoy, K. G. Heiple, A. H. Burstein, *Am. J. Phys. Anthropol.* **38**, 757 (1973).
18. M. Nakatsukasa, M. Pickford, N. Egi, B. Senut, *Primates* **48**, 171 (2007).
19. We use "australopith" as a vernacular term to refer to *Australopithecus* and *Paranthropus* species, following (1).
20. F. A. Jenkins, *Science* **178**, 877 (1972).
21. J. T. Stern Jr., R. L. Susman, *Am. J. Phys. Anthropol.* **55**, 153 (1981).
22. C. B. Ruff, in *Primate Locomotion: Recent Advances*, E. Strasser, J. G. Fleagle, A. Rosenberger, H. M. McHenry, Eds. (Plenum, New York, 1998), pp. 449–469.
23. T. D. White *et al.*, *Nature* **440**, 883 (2006).
24. C. B. Ruff, *Am. J. Phys. Anthropol.* **98**, 527 (1995).
25. B. G. Richmond, L. C. Aiello, B. A. Wood, *J. Hum. Evol.* **43**, 529 (2002).
26. D. R. Carrier, *Curr. Anthropol.* **25**, 483 (1984).
27. W. L. Jungers, *J. Hum. Evol.* **17**, 247 (1988).
28. K. L. Steudel-Numbers, *J. Hum. Evol.* **51**, 445 (2006).
29. M. D. Sockol, D. A. Raichlen, H. Pontzer, *Proc. Natl. Acad. Sci. U.S.A.* **104**, 12265 (2007).
30. B. G. Richmond, D. R. Begun, D. S. Strait, *Yrbk. Phys. Anthropol.* **116**, 70 (2001).
31. S. K. Thorpe, R. L. Holder, R. H. Crompton, *Science* **316**, 1328 (2007).
32. C. O. Lovejoy, R. S. Meindl, J. C. Ohman, K. G. Heiple, T. D. White, *Am. J. Phys. Anthropol.* **119**, 97 (2002).
33. J. T. J. Stern Jr., R. L. Susman, *Am. J. Phys. Anthropol.* **60**, 279 (1983).
34. J. T. J. Stern Jr., *Evol. Anthropol.* **9**, 113 (2000).

35. This research was supported by The George Washington University, Stony Brook University, and the NSF. We gratefully acknowledge the assistance of the curators at the numerous institutions housing the extant and fossil collections used in this study. We also thank M. Pickford and B. Senut for helpful discussions, and B. Wood,

J. Stern, D. Strait, M. Nakatsukasa, and the anonymous reviewers for constructive comments on our manuscript.

#### Supporting Online Material

www.sciencemag.org/cgi/content/full/319/5870/1662/DC1  
Materials and Methods

Figs. S1 to S6  
Tables S1 to S3  
References

14 December 2007; accepted 22 February 2008  
10.1126/science.1154197

# Activation of FOXO1 by Cdk1 in Cycling Cells and Postmitotic Neurons

Zengqiang Yuan,<sup>1,\*</sup> Esther B. E. Becker,<sup>1,\*</sup> Paola Merlo,<sup>1</sup> Tomoko Yamada,<sup>1</sup> Sara DiBacco,<sup>1</sup> Yoshiyuki Konishi,<sup>1</sup> Erik M. Schaefer,<sup>2</sup> Azad Bonni<sup>1,†</sup>

Activation of cyclin-dependent kinase 1 (Cdk1) has been linked to cell death of postmitotic neurons in brain development and disease. We found that Cdk1 phosphorylated the transcription factor FOXO1 at Ser<sup>249</sup> in vitro and in vivo. The phosphorylation of FOXO1 at Ser<sup>249</sup> disrupted FOXO1 binding with 14-3-3 proteins and thereby promoted the nuclear accumulation of FOXO1 and stimulated FOXO1-dependent transcription, leading to cell death in neurons. In proliferating cells, Cdk1 induced FOXO1 Ser<sup>249</sup> phosphorylation at the G<sub>2</sub>/M phase of the cell cycle, resulting in FOXO1-dependent expression of the mitotic regulator Polo-like kinase (Plk). These findings define a conserved signaling link between Cdk1 and FOXO1 that may have a key role in diverse biological processes, including the degeneration of postmitotic neurons.

The protein kinase Cdk1 is a key mediator of neuronal cell death that is relevant to brain development and degeneration (1–6). As a major apoptotic kinase, Cdk1 might be expected to orchestrate a program of gene expression that activates the cell death machinery. Because Cdk1 resides in the cytoplasm in neurons (1, 5, 6), we reasoned that Cdk1 might regulate gene expression through proteins that shuttle between the cytoplasm and nucleus. The FOXO transcription factors undergo nucleocytoplasmic shuttling and control cell death (7, 8). We therefore investigated the role of FOXO proteins in propagating the Cdk1 cell death signal to the nucleus in postmitotic neurons.

FOXO1 contains a conserved putative Cdk1 phosphorylation site within the forkhead domain at Ser<sup>249</sup> (fig. S1A). Cdk1 catalyzed the phosphorylation of FOXO1 in vitro (Fig. 1A) (9). Cdk1 also phosphorylated the FOXO1 forkhead domain (FOXO1FD) in vitro, but failed to phosphorylate a FOXO1FD mutant in which Ser<sup>249</sup> was replaced with alanine (FOXO1FD S249A) (fig. S1B). We generated an antibody that specifically recognizes FOXO1 that is phosphorylated at Ser<sup>249</sup> (9). The phosphoS249-FOXO1 antibody recognized recombinant FOXO1 or FOXO1FD that was phosphorylated by Cdk1 in vitro but did not recognize unphosphorylated

FOXO1 or the FOXO1FD S249A mutant that was incubated with Cdk1 in vitro (Fig. 1B and fig. S1C). We expressed cyclin B and Cdk1 in 293T cells together with FOXO1 or a S249A FOXO1 mutant. Immunoblotting of total lysates or FOXO1 immunoprecipitates of transfected cells revealed that Cdk1 increased the amount of phosphorylated FOXO1 at Ser<sup>249</sup> in cells (Fig. 1C and fig. S1D). In other experiments, depletion of endogenous Cdk1 by RNA interference (RNAi) reduced the FOXO1 phosphorylation in cells (Fig. 1D

and fig. S1E), which suggested a requirement for endogenous Cdk1 in the FOXO1 phosphorylation at Ser<sup>249</sup> in cells.

We tested whether the activation of endogenous Cdk1 induced the phosphorylation of endogenous FOXO1 at Ser<sup>249</sup> in neurons. Endogenous Cdk1 is activated in cerebellar granule neurons upon inhibition of membrane depolarization (1, 3). We found that the amount of FOXO1 Ser<sup>249</sup> phosphorylation was higher in neurons deprived of membrane-depolarizing concentrations of KCl (5 mM KCl) than in neurons maintained in depolarizing medium (30 mM KCl) (Fig. 1E). The Cdk1 inhibitor roscovitine reduced the FOXO1 Ser<sup>249</sup> phosphorylation in neurons deprived of depolarization (Fig. 1E). Thus, endogenous Cdk1 appears to mediate activity deprivation-induced phosphorylation of endogenous FOXO1 at Ser<sup>249</sup> in neurons.

The identification of Cdk1-induced phosphorylation of FOXO1 at Ser<sup>249</sup> led us to test whether the FOXO1 phosphorylation mediated the ability of Cdk1 to trigger cell death in neurons. Because endogenous Cdk1 is required for apoptosis of activity-deprived neurons (1, 3), we determined the role of FOXO1 in apoptosis of neurons deprived of activity. We transfected neurons with the U6/foxo RNAi or control U6 plasmid. FOXO RNAi reduced the expression of FOXO1 in primary granule neurons and

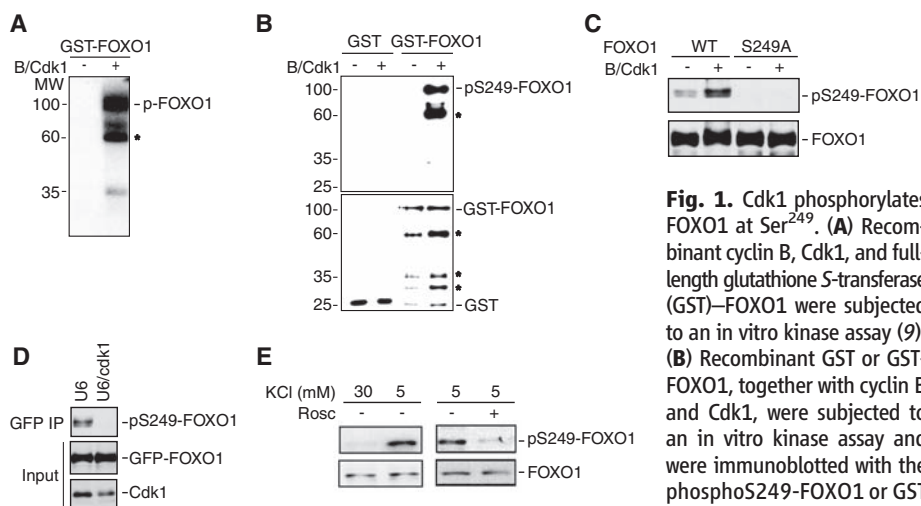


**Fig. 1.** Cdk1 phosphorylates FOXO1 at Ser<sup>249</sup>. (A) Recombinant cyclin B, Cdk1, and full-length glutathione S-transferase (GST)-FOXO1 were subjected to an in vitro kinase assay (9). (B) Recombinant GST or GST-FOXO1, together with cyclin B and Cdk1, were subjected to an in vitro kinase assay and were immunoblotted with the phosphoS249-FOXO1 or GST antibody. Asterisks indicate GST-

<sup>1</sup>Department of Pathology, Harvard Medical School, 77 Avenue Louis Pasteur, Boston, MA 02115, USA. <sup>2</sup>Center for Signal Transduction, Cellular Analysis Business Unit/BioDiscovery Division, Invitrogen Corporation, 94 South Street, Hopkinton, MA 01748, USA.

\*These authors contributed equally to this work.

†Present address: Institute of Biophysics, Chinese Academy of Sciences, 15 Datun Road, Beijing 100101, China.

‡To whom correspondence should be addressed. E-mail: azad\_bonni@hms.harvard.edu

FOXO1 degradation products. (C) Lysates of 293T cells transfected with cyclin B and Cdk1 or the control vector, together with the green fluorescent protein (GFP) fusion protein GFP-FOXO1 or the GFP-FOXO1 S249A mutant, were immunoblotted with the phosphoS249-FOXO1 antibody or a mouse monoclonal FOXO1 antibody. (D) Lysates of Neuro2A cells transfected with the control U6 or U6/cdk1 RNAi plasmid and GFP-FOXO1 were immunoprecipitated with the GFP antibody and immunoblotted with the phosphoS249-FOXO1 antibody. Lysates were also immunoblotted with the GFP or Cdk1 antibody. (E) Lysates of granule neurons maintained in membrane-depolarizing medium (30 mM KCl) or in which depolarization was inhibited (5 mM KCl) in the presence of the Cdk1 inhibitor roscovitine (10  $\mu$ M) or its vehicle [dimethyl sulfoxide (DMSO)] were immunoblotted with the phosphoS249-FOXO1 or FOXO1 antibody.